CU Journal of Non-Linear Fluid Mechanics
Vol. 01, No. 01, 2025
https://doi.org/10.11615/cujnlfm.01102-6

Thermal Analysis of a Reactive Third-Grade Fluid Film Flow on a Vertically Moving Heated Belt

Oluwole Daniel Makinde[*a] and Micheal H. Mkwizu[b]
[a]Faculty of Military Science, Stellenbosch University, Private Bag X2, Saldanha 7395, South Africa.
[b]Department of Mathematics, Informatics and Computational Sciences, Solomon Mahlangu College of Science and Education, Sokoine University of Agriculture, Tanzania.

Abstract

Real-world engineering and industrial processes such as film casting, extrusion, lubrication, and coating, where precise control of heat transfer and reaction kinetics is essential for achieving efficiency and maintaining product quality. Analyzing this complex system facilitates the optimization of key parameters, including belt velocity, heat flux, and reaction rates, to enhance thermal efficiency, and mitigate safety risks such as thermal runaway in reactive environments. This study investigates the thermal stability of a reactive third-grade fluid thin film flow on a heated moving belt with an adiabatic-free surface. It assumes an exothermic reaction based on Arrhenius kinetics while ignoring material consumption. The coupled system of nonlinear ordinary differential equations is solved using a perturbation approach combined with a specialized Hermite–Pade´ approximation technique. Results indicate that fluid velocity peaks at the moving belt and diminishes toward the free surface, whereas fluid temperature reaches its maximum at the free surface. Furthermore, increasing the moving belt parameter accelerates thermal criticality, leading to an earlier onset of thermal runaway, highlighting the need for careful parameter optimization to enhance thermal efficiency and mitigate safety risks in such reactive systems. The moving heated belt acts as a dynamic boundary condition, effectively replicating

Keywords: Moving belt; Reactive third grade fluid; Hermite–Pade´ approximants; Thermal analysis.

Nomenclature

(x, y)	coordinate system	(m)	Q	heat of reaction	(kJ/mol)
v	fluid velocity	(m/s)	R	universal gas constant	(J/kg K)
C_0	concentration of the reactant	(mol/L)	U_0	belt constant velocity	(m/s)
A	rate constant	-	T	fluid temperature	(K)
E	activation energy	(kJ/mol)	g	gravitational acceleration	(m/s^2)
k	thermal conductivity	(W/m-K)	T_0	belt temperature	(K)

* ✉ makinded@cput.ac.za

m	viscous heating parameter	-	G	moving belt parameter	-
W	dimensionless velocity	-			
GREEK SYMBOLS					
μ	fluid dynamics viscosity	(kg/sm)	ε	activation energy parameter	-
λ	Frank-Kamenetskii parameter	-	δ	thin film thickness	-
θ	dimensionless temperature	-	β_3	material coefficient	-
ρ	fluid density	(kg/m^3)	γ	dimensionless non-Newtonian parameter	-

1 Introduction

The heat transfer analysis of non-Newtonian fluid film flow over a vertically moving heated belt is pivotal for optimizing industrial processes and ensuring high-quality products. Non-Newtonian fluids possess temperature-sensitive rheological properties, such as viscosity and elasticity, making thermal management essential for maintaining flow stability and uniform film thickness [1]. The moving heated belt serves as a dynamic boundary condition that replicates real-world applications such as film casting, extrusion, and coating, where precise control of heat transfer and reaction kinetics is critical to process efficiency and product quality [2]. This analysis facilitates the optimization of key parameters, including belt velocity, heat flux, and reaction rates, to enhance thermal efficiency, ensure uniform temperature distribution, and mitigate risks like thermal runaway in reactive systems. Applications span a variety of industries, from polymer and composite material production to food processing, pharmaceutical film formation, and advanced energy systems, where non-Newtonian fluids are integral to cooling, shaping, and coating processes [3, 4]. By addressing heat dissipation and thermal stresses, this study contributes to safer, more energy-efficient, and higher-quality industrial processes, highlighting its importance in modern engineering research.

Several studies have explored various aspects of non-Newtonian thin-film flows on moving heated belts. Makinde [5] investigated the gravity-driven flow of non-Newtonian thin films along heated inclined plates, addressing irreversibilities and providing approximate analytical solutions using the perturbation method. Siddiqui et al. [6] examined the flow behaviour of Sisko and Oldroyd six-constant fluid films over a moving belt, using the Homotopy Perturbation Method (HPM) to derive velocity profiles and analyze flow dynamics. Nemati et al. [7] studied heat transfer and flow stability in Sisko and Oldroyd fluid films on vertical belts, employing the Homotopy Analysis Method (HAM) to reveal the impact of auxiliary parameters on fluid stability and film thickness. Gul et al. [8] provided exact solutions for two immiscible non-Newtonian fluids forming a thin film on a vertical moving belt, with a focus on power-

law fluid models and interlayer interactions. Rahim et al. [9] developed analytical models for the flow of modified second-grade fluid films, highlighting the influence of heat transfer and shear rate dependence on industrial processes. Moosavi et al. [10] applied the variational iteration method to thin-film flows of non-Newtonian fluids, illustrating the effects of temperature variations under high-shear conditions. Gul et al. [11] explored magnetohydrodynamic (MHD) thin-film flows of third-grade fluids, investigating the interplay between magnetic fields, heat flux, and boundary conditions on vertical belts. Sahoo et al. [12] used finite element methods to study the stability and thermal dynamics of thin-film flows, emphasizing the role of belt speed and fluid rheology. Sharma et al. [13] examined viscoelastic properties in non-Newtonian fluid flows over vertical moving belts, combining analytical and numerical approaches to provide insights into the influence of rheological parameters on flow dynamics. Ashraf et al. [14] analyzed heat transfer in Johnson–Segalman fluid films over heated belts, demonstrating how temperature-dependent viscosity affects film thickness, particularly in polymer coating processes. Additional studies relevant to this work can be found in [15, 16].

To the best of the author's knowledge, no prior studies have specifically investigated the thermal analysis of a reactive third-grade fluid film flow over a vertically moving heated belt. Such an analysis is crucial for understanding the complex interplay between non-Newtonian fluid dynamics, heat transfer, and chemical reactions [17, 18], which play a significant role in various industrial applications. Third-grade fluids, characterized by their shear-thinning or shear-thickening behaviour, are commonly encountered in processes such as polymer manufacturing, chemical coating applications, and lubrication systems. The addition of a chemically reactive component further complicates the system, as exothermic reactions significantly influence flow stability and temperature distribution. This unexplored area underscores the need for further research to better understand the dynamics of these fluids and develop accurate models for engineering applications. In this study, the authors address this research gap by employing the perturbation method and specialized Hermite-Padé approximants ([19, 20]) to solve the coupled nonlinear ordinary differential equations (ODEs) governing the system. The subsequent sections present the problem formulation, detailed analysis, and solution approach. Results are displayed graphically and quantitatively analyzed with respect to various system parameters.

2 Mathematical model

We consider a container filled with an incompressible reactive third-grade non-Newtonian fluid. A wide heated belt with a constant velocity of U_0 moves vertically upward through the container. As depicted in Figure 1, the (x, y)-coordinate system is chosen such that the x-axis is normal to the heated belt, and the y-axis is along the belt in the upward direction. Since the belt moves upward and passes through the fluid, it picks up a film fluid of thickness δ. Due to gravity, the reactive fluid film tends to drain down the belt. For simplicity, the following assumptions are made:

(i) The flow is in a steady state.

(ii) The flow is laminar and uniform.

(iii) The film fluid thickness δ is uniform with an adiabatic-free surface.

(iv)The belt temperature T_0 is uniform.

The only velocity component $v(x)$ is in the y-direction, therefore, under these conditions, the governing momentum and energy balance equations take the form [6-12];

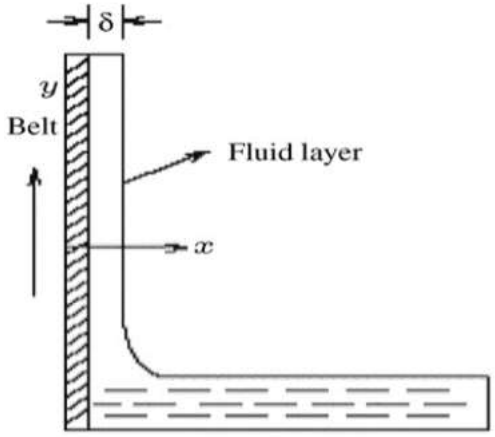

Figure 1: Geometry of the problem.

$$\mu\frac{d^2v}{dx^2}+6\beta_3\frac{d^2v}{dx^2}\left(\frac{dv}{dx}\right)^2-\rho g=0, \tag{1}$$

$$k\frac{d^2T}{dx^2}+\left(\frac{dv}{dx}\right)^2\left(\mu+2\beta_3\left(\frac{dv}{dx}\right)^2\right)+QC_0Ae^{-\frac{E}{RT}}=0, \tag{2}$$

subject to the boundary conditions:

$$\frac{dv}{dx}=0,\quad \frac{dT}{dx}=0,\qquad \text{on}\qquad x=\delta, \tag{3a}$$

$$v=U_0,\ T=T_0,\qquad \text{on}\qquad x=0, \tag{3b}$$

where the additional Arrhenius kinetics term in the energy balance equation is due to the exothermic reaction within the fluid [10]. Here T is the absolute temperature, δ is the thin film thickness, ρ is the fluid density, g is the gravitational acceleration, k is the thermal conductivity of the material, Q is the heat of reaction, A is the rate constant, E is the activation energy, R is the universal gas constant, C_0 is the initial concentration of the reactant species, β_3 is the material coefficient and μ is the dynamic viscosity coefficient. It is important to note that the model equations (1)-(2) together with the moving heated belt and adiabatic thin-film free surface boundary conditions in equations (3a,b), effectively replicate real-world engineering and industrial processes

such as film casting, extrusion, lubrication, and coating, where precise control of heat transfer and reaction kinetics is essential for achieving efficiency and maintaining product quality. We introduce the following dimensionless variables into equations (1)-(3);

$$\theta = \frac{E(T-T_0)}{RT_0^2}, \quad \bar{x} = \frac{x}{\delta}, \quad \lambda = \frac{QEA\delta^2 C_0 e^{-\frac{E}{RT_0}}}{T_0^2 Rk}, W = \frac{v}{U_0},$$
$$m = \frac{\mu U_0^2 e^{\frac{E}{RT_0}}}{QA\delta^2 C_0}, \varepsilon = \frac{RT_0}{E}, \gamma = \frac{\beta_3 U_0^2}{\mu\delta^2}, G = \frac{\rho g \delta^2}{\mu U_0}, \tag{4}$$

and obtain the dimensionless governing equation together with the corresponding boundary conditions (neglecting the bar symbol for clarity);

$$\frac{d^2W}{dx^2} + 6\gamma \frac{d^2W}{dx^2}\left(\frac{dW}{dx}\right)^2 = G, \tag{5}$$

$$\frac{d^2\theta}{dx^2} + \lambda\left[e^{\left(\frac{\theta}{1+\varepsilon\theta}\right)} + m\left(\frac{dW}{dx}\right)^2\left(1+2\gamma\left(\frac{dW}{dx}\right)^2\right)\right] = 0, \tag{6}$$

with

$$\frac{dW}{dx} = 0, \quad \frac{d\theta}{dx} = 0, \qquad \text{on} \qquad x = 1, \tag{7a}$$

$$W = 1, \quad \theta = 0, \qquad \text{on} \qquad x = 0, \tag{7b}$$

where G, λ, ε, γ, and m represent the moving belt parameter, the Frank-Kamenetskii parameter, the activation energy parameter, the dimensionless non-Newtonian parameter, and the viscous heating parameter, respectively. In the following sections, equations (5)-(7) are solved using both perturbation and multivariate series summation techniques [19, 20].

3 Perturbation method

Due to the nonlinear nature of the velocity and temperature fields equations (5)-(7), it is convenient to form a power series expansion both in the dimensionless non-Newtonian parameter γ and the Frank-Kamenetskii parameter λ, i.e.,

$$W = \sum_{i=0}^{\infty} W_i \gamma^i, \quad \theta = \sum_{i=0}^{\infty} \theta_i \lambda^i. \tag{8}$$

Substituting the solution series in equation (8) into equations (5)-(7) and collecting the coefficients of like powers of γ and λ, we obtained and solved the equations for the coefficients of the solution series iteratively. The solutions for the velocity and temperature fields are given as;

$$W(x)=1+\frac{1}{2}G(x^2-2x)-\frac{1}{2}G^3x(x-2)(x^2-2x+2)\gamma+2G^5x(x-2)(x^2-x+1)(x^2-3x+3)\gamma^2 \\ -12G^7x(x-2)(x^2-2x+2)(x^4-4x^3+6x^2-4x+2)\gamma^3+O(\gamma^4) \quad (9)$$

$$\theta(x) = -\frac{1}{60060}x(-2+x)(30030 - 28028mx^2G^4\gamma + 5005x^2G^2 - 10010xmG^2 - 174720mG^{10}\gamma^4 + 160160mG^8\gamma^3 - 12012mG^4\gamma - 51480mG^6\gamma^2 + 73920mG^{12}\gamma^5 + 10010mG^2 - 283140mx^2G^6\gamma^2 - 242800mx^9G^{12}\gamma^5 - 1985984mx^5G^8\gamma^3 + 77220mx^5G^6\gamma^2 + 9143680mx^5G^{10}\gamma^4 - 4435200mx^3G^{12}\gamma^5 + 308880mx^3G^6\gamma^2 + 2754752mx^4G^8\gamma^3 + 8352960mx^4G^{12}\gamma^5 + 1601600mx^2G^8\gamma^3 - 2562560mx^3G^8\gamma^3 + 3727360mx^7G^{10}\gamma^4 - 205920mx^4G^6\gamma^2 - 2766400mx^2G^{10}\gamma^4 + 928928mx^6G^8\gamma^3 - 12870mx^6G^6\gamma^2 - 256256mx^7G^8\gamma^3 - 8619520mx^4G^{10}\gamma^4 + 32032mx^9G^8\gamma^3 + 5712960mx^8G^{12}\gamma^5 - 9715200mx^7G^{12}\gamma^5 - 6959680mx^6G^{10}\gamma^4 - 126720mx^{11}G^{12}\gamma^5 + 16016mx^3G^4\gamma + 291200mx^9G^{10}\gamma^4 + 5824000mx^3G^{10}\gamma^4 + 707520mx^8G^{10}\gamma^4 - 4004mx^4G^4\gamma + 1700160mx^2G^{12}\gamma^5 + 10560mx^{12}G^{12}\gamma^{12} - 1339520mx^8G^{10}\gamma^4 - 29120mx^{10}G^{10}\gamma^4 - 11679360mx^5G^{12}\gamma^5 + 12281280mx^6G^{12}\gamma^5 - 443520mxG^{12}\gamma^5 + 154440xmG^6\gamma^2 + 24024xmG^4\gamma - 640640xmG^8\gamma^3 + 873600xmG^{10}\gamma^4)\lambda + O(\lambda^2). \quad (10)$$

By utilizing a computer symbolic algebra package (MAPLE), we computed the first nineteen terms of the solution series for equations (9) - (10). While these power series solutions are valid only for very small parameter values, we have extended their applicability to larger parameter values using the Hermite-Padé approximation technique, as demonstrated in the following section. The key physical quantities of interest in this problem are the skin-friction parameter (C_f) and the Nusselt number (Nu), which are defined by

$$C_f = \frac{\delta\iota_w}{\mu U_0} = \frac{dW}{dx}(0), \quad Nu = \frac{\delta E q_w}{kRT_0^2} = -\frac{d\theta}{dx}(0), \quad (11)$$

where $\iota_w = \mu dv/dx$ and $q_w = -kdT/dx$ are the shear stress and the heat flux evaluated at the surface of the moving belt (i.e. $x = 0$) respectively.

4 Thermal criticality and bifurcation study

To identify the onset of thermal criticality in the system, we utilize a specialized Hermite-Padé approximation technique. Let's assume that the partial sum

$$U_{N-1}(\lambda) = \sum_{i=0}^{N-1} a_i \lambda^i = U(\lambda) + O(\lambda^N) \text{ as } \lambda \to 0, \quad (12)$$

is given [19, 20]. It is important to note that equation (12) can be applied to approximate any output of the solution to the problem under investigation, such as the skin friction (C_f) and the surface heat flux (Nu), since all quantities can be expanded as a Taylor series in the given small parameter. Assume $U(\lambda)$ is a local representation of an algebraic function of λ in the context of nonlinear problems. Thus, we seek an expression of the form

$$F_d(\lambda, U_{N-1}) = A_{0N}(\lambda) + A_{1N}^d(\lambda)U^{(1)} + A_{2N}^d(\lambda)U^{(2)} + A_{3N}^d(\lambda)U^{(3)}, \quad (13)$$

such that

$$A_{0N}(\lambda)=1,\ A_{iN}^d(\lambda) = \sum_{j=1}^{d+i} b_{ij}\lambda^{j-1}\ , \quad (14)$$

and

$$F_d(\lambda, U) = O(\lambda^{N+1}) \quad \text{as } \lambda \to 0, \quad (15)$$

where $d \geq 1$, i =1, 2, 3. The condition in equation (14) normalizes F_d and ensures that the order of the series A_{iN}^d increases as i and d increase. Consequently, there are 3(2+d) undetermined coefficients b_{ij} in the equation (14). The requirement in equation (15) simplifies the problem to a system of N linear equations for the unknown coefficients of F_d. The entries of the underlying matrix depend solely on the N given coefficients a_i. From this point forward, we shall take

$$N=3(2+d). \quad (16)$$

This ensures that the number of equations matches the number of unknowns. Equation (16) provides the condition for selecting the values of d, and it's important to note that d depends on the N coefficients of the available partial sum. Equation (15) introduces a new special type of Hermite-Padé approximants. For example, we let

$$U^{(1)}=U,\quad U^{(2)}=U^2,\quad U^{(3)}=U^3, \quad (17)$$

and obtain a cubic Padé approximant. This allows us to identify additional solution branches of the underlying problem beyond the one represented by the original series. Similarly, we can proceed by setting

$$U^{(1)}=U,\quad U^{(2)}=DU,\quad U^{(3)}=D^2U, \quad (18)$$

in equation (15), where D is the differential operator given by $D=d/d\lambda$. This results in second-order differential approximants and allows us to determine the dominant singularity in the flow field i.e. by equating the coefficient $A_{3N}(\lambda)$ of the equation (18) to zero. Meanwhile, it is crucial to understand that the choice of the degrees of A_{iN} in equation (13) for this application is based on a straightforward technique for determining singularities in second-order linear ordinary differential equations with polynomial coefficients, as well as the potential for multiple solution branches in the nonlinear problem [19]. In practice, the dominant singularities are typically found at the zeros of the leading polynomial coefficients ($A_{3N}^{(d)}$) of the second-order linear ordinary differential equation in equation (18). According to [20], it is well established that the dominant behaviour of any solution output to the differential equation can be characterized for some values of α and H as follows:

$$U(\lambda) \approx \begin{cases} H(\lambda_C - \lambda)^{\alpha} & \text{for} \quad \alpha \neq 0,1,2,... \\ H(\lambda_C - \lambda)^{\alpha} \ln|\lambda_C - \lambda| & \text{for} \quad \alpha = 0,1,2,... \end{cases} \quad \text{as } \lambda \to \lambda_C \qquad (19)$$

where H is a constant and λ_c is the critical point with the exponent α. The critical exponent α_N can be readily determined using Newton's polygon algorithm. Assuming an algebraic-type singularity as given in equation (19), the exponent can be approximated by

$$\alpha_N = 1 - \frac{A_{2N}(\lambda_{CN})}{DA_{3N}(\lambda_{CN})} \ . \qquad (20)$$

It is well established that for algebraic equations, the only structurally stable singularities are simple turning points. Therefore, in practice, one nearly always finds $\alpha_N = 1/2$.

5 Results and discussion

This study examines the thin film flow of a reactive third-grade fluid over a vertically moving belt, focusing on its heat transfer characteristics. This subsection aims to analyze the numerical results for velocity and temperature distributions, skin friction, and the Nusselt number, along with bifurcation profiles. The influence of various embedded parameters is explored, with results presented in Tables 1–2 and Figures 2–7. The bifurcation procedure described in Section 4 was applied to the first nineteen terms of the solution series, yielding the results presented in Tables 1 and 2 below

Table 1: Computations showing rapid convergence and bifurcation point in the velocity field ($G = 1$).

d	N	C_f	γ_c	α_{cN}
1	9	-1.500191067753	-0.074077212118	0.4999870
2	12	-1.500000000000	-0.074074074074	0.5000000
3	15	-1.500000000000	-0.074074074074	0.5000000
4	18	-1.500000000000	-0.074074074074	0.5000000

Table 2: Computations showing thermal criticality for different parameter values

m	G	γ	$Nu(\varepsilon = 0)$	$\lambda_c\ (\varepsilon = 0)$	α_{cN}
1.0	0.1	0.0	2.002783645	0.8778465618	0.50000
1.0	0.1	0.1	2.002780204	0.8778470646	0.50000

1.0	0.1	0.2	2.002776733	0.8778475707	0.50000
1.0	0.1	0.3	2.002773233	0.8778480800	0.50000
1.0	0.2	0.1	2.011056222	0.8760288700	0.50000
1.0	0.3	0.1	2.024631106	0.8730439477	0.50000

The reactive third-grade fluid under investigation is assumed to be highly combustible, with large activation energy (i.e., $\varepsilon = 0$). The results in Table 1 demonstrate the rapid convergence of our method concerning the non-Newtonian parameter (γ_c), the dominant singularity, and its critical exponent (α_c) as the number of series coefficients used in the approximants gradually increases. A bifurcation point, or turning point, occurs in the flow field at $(\gamma_c, C_f) = (-2/27G^2, -3G/2)$, as illustrated in Fig. 6. Table 2 shows that the magnitude of thermal criticality (λc) increases with the value of the non-Newtonian parameter and decreases with an increasing value of the moving belt parameter (G). This indicates that increased belt motion may lead to an earlier onset of the thermal runaway phenomenon, while a higher non-Newtonian parameter can enhance thermal stability. Furthermore, determining the thermal criticality values in a reactive third-grade thin film flow over a vertically moving belt is essential for ensuring safety, efficiency, and reliability in engineering and industrial applications. It helps prevent runaway reactions and overheating, ensuring that processes such as film casting, extrusion, lubrication, and coating operate within safe thermal limits. Understanding thermal criticality allows engineers to design effective heat management systems, select appropriate materials, and optimize energy usage, reducing waste and improving overall process efficiency. Additionally, it ensures scalability, consistent product quality, and compliance with environmental regulations by controlling emissions and waste heat. Ultimately, thermal criticality analysis is vital for maintaining safe, sustainable, and high-performance operations in industries that rely on reactive thin film flows.

Figs. 2 and 3 depict the variation of the fluid velocity field, generally showing a transverse decrease in fluid velocity, with the maximum at the moving belt and the minimum at the fluid's free surface. The figures further illustrate that velocity increases with an increase in γ and decreases with an increase in G. Figs. 4 and 5 show a transverse increase in fluid temperature, peaking at the free surface. It is noteworthy that fluid temperature rises with increasing values of both the moving belt parameter (G) and the Frank-Kamenetskii parameter (λ), due to Arrhenius kinetics. Fig. 7 presents a slice of the bifurcation diagram for $\gamma > 0$ in the (λ, Nu) plane, illustrating the variation of moving belt surface heat flux (Nu) with the Frank-Kamenetskii parameter (λ). Notably, there is a critical value λc (a turning point), where for $0 \leq \lambda < \lambda_c$, there are two solutions (labeled I and II). These upper and lower solution branches arise due to Arrhenius kinetics in the governing thermal boundary layer equation (Eq. 2). For $\lambda > \lambda_c$, the system has no real solution, displaying a classical form indicative of thermal runaway.

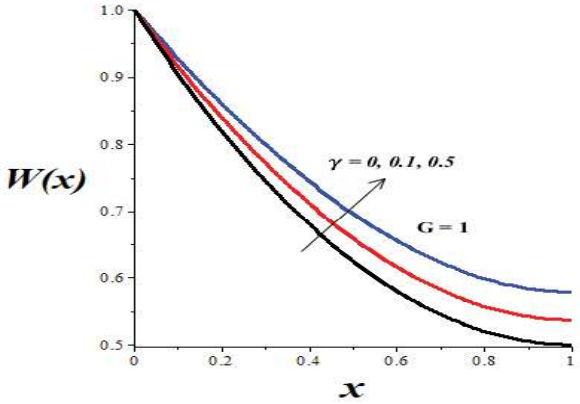

Figure 2: Impact of γ on the velocity profiles.

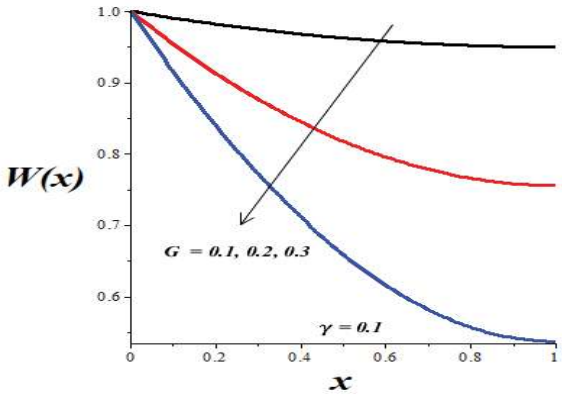

Figure 3: Impact of G on velocity profiles.

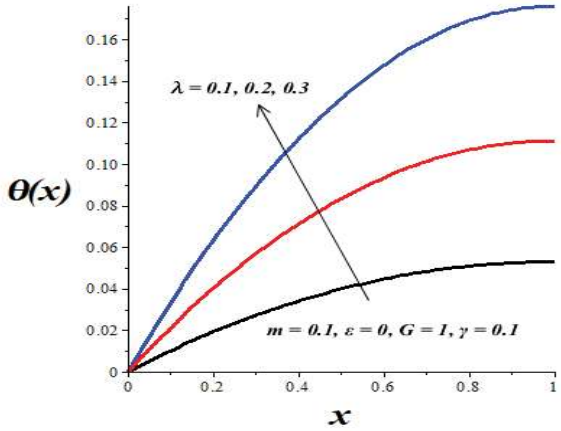

Figure 4: Impact of λ on temperature profiles.

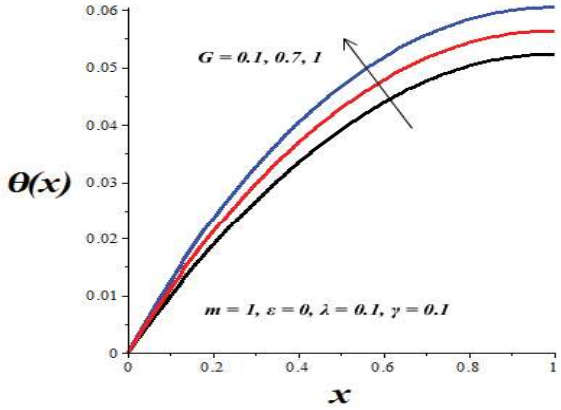

Figure 5: Impact of G on temperature profiles.

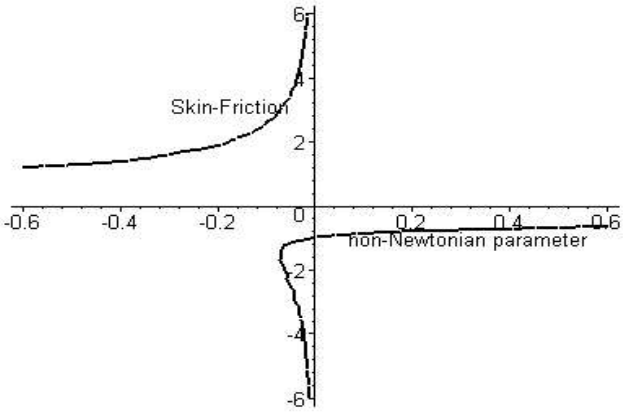

Figure 6: A slice of bifurcation diagram in the (γ, C_f) plane (G = 1).

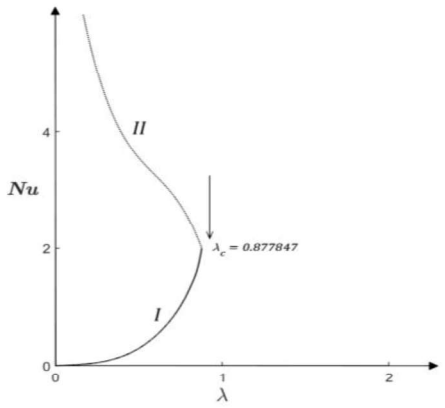

Figure 7: A slice of approximate bifurcation diagram in the (λ , Nu(m = 1, γ = 0.1, G = 0.1, ε = 0)) plane.

5 Conclusions

This paper investigates the hydrodynamically and thermally developed flow of a reactive third-grade liquid film along an upward-moving vertical heated belt with an adiabatic-free surface. The fluid velocity is found to peak near the moving belt and diminish toward the free surface, while the maximum temperature is observed at the free surface. Using a specialized Hermite-Padé approximation method, the thermal criticality conditions and multiple solution branches are accurately determined. The study reveals that increasing the moving belt parameter accelerates the onset of thermal runaway within the system. Furthermore, the findings of this study contribute to preventing overheating, ensuring energy efficiency, and mitigating risks associated with reactive third-grade fluid film flows, making it invaluable for designing safer and more efficient systems in chemical, textile, and material processing industries. The semi-numerical Hermite-Padé approximation approach also demonstrates its effectiveness in solving other parameter-dependent, highly nonlinear boundary-value problems in science and engineering. Future research could extend this study by considering the combined effects of physical factors such as magnetic fields, Joule heating, thermal radiation, convective heating, and embedded porous media on reactive non-Newtonian fluid film flows over a vertically moving heated belt.

References

[1] Schowalter W. R., *Mechanics on Non-Newtonian Fluids.* Pergamon Press, 1978.
[2] Rossum J. J. V., "Viscous lifting and drainage of liquid", *Applied Scientific Research*, vol. 7, pp. 141–145, 1958.
[3] Wylie J. J. and Huang H., "Extensional flows with viscous heating", *Journal of Fluid Mechanics,* vol. 571, pp. 359–370, 2007.
[4] O'Brien S. B. G. and Schwartz L.W., "Theory and modeling of thin film flow", *Encyclopedia of Surface and Colloid Science*, vol. 01, pp. 5283–5297, 2002.

[5] Makinde O. D., "Irreversibility analysis for gravity-driven non-Newtonian liquid film along an inclined isothermal plate", *Physica Scripta*, vol. 74, pp. 642—645, 2006.

[6] Siddiqui A. M., Ahmed M., and Ghori Q. K., "Thin film flow of non-Newtonian fluids on a moving belt", *Chaos, Solitons & Fractals*, vol. 33, pp. 1107–1118, 2007.

[7] Nemati H., Ghanbarpour M., and Khademi M., "Thin film flow of non-Newtonian fluids on a vertical moving belt using Homotopy Analysis Method", *Journal of Engineering Science and Technology Review,* vol. 2(1), pp. 118—122, 2009.

[8] Gul T., Shah R. A., Islam S., Ullah M., and Khan M. A., "Exact solution of two thin film non-Newtonian immiscible fluids on a vertical belt", *Journal of Basic and Applied Scientific Research*, vol. 4(6), pp. 283—288, 2014.

[9] Rahim M., Khan Z. H., and Malik M. Y., "Analytical solutions for thin film flow of modified second-grade fluids over a vertical moving belt with heat transfer", *International Journal of Heat and Mass Transfer,* vol. 70(1), pp. 564–573, 2014.

[10] Moosavi M., Momeni M., and Tavangar T., "Variational iteration method for flow of non-Newtonian fluid on a moving belt and in a collector", *Alexandria Engineering Journal,* vol. 55(3), pp. 2759–2770, 2016.

[11] Gul T., Shah R. A., Islam S., Ghani F., and Khan I., "MHD thin film flows of a third-grade fluid on a vertical belt with slip boundary conditions", *Journal of Propulsion and Power Engineering,* vol. 2(1), pp. 35–45, 2016.

[12] Sahoo M., Gupta R., and Saini K., "Stability analysis of non-Newtonian fluid flow on a moving belt", *Applied Mathematics and Computation,* vol. 320, pp. 384–396, 2018.

[13] Sharma N., Kumar A., and Joshi M., "Thin film flow of viscoelastic fluids: Numerical and analytical study", *Journal of Non-Newtonian Fluid Mechanics*, vol. 285, p. 104361, 2020.

[14] Ashraf H., Sabir S., Siddiqui A. M., and Rehman H. U., "Heat transfer analysis of temperature-dependent viscosity Johnson–Segalman fluid film flow on a vertical heated belt", *Case Studies in Thermal Engineering*, vol. 44, p. 103961, 2023.

[15] Makinde O. D., "Laminar falling liquid film with variable viscosity along an inclined heated plate, *Applied Mathematics and Computation"*, vol. 175, pp. 80—88, 2006.

[16] Khan Z., Tairan N., Mashwani W. K., Rasheed H. U., Shah H., and Khan W., "MHD and slip effect on two-immiscible third grade fluid on thin film flow over a vertical moving belt", *Open Physics,* vol. 17(1), pp. 575–586, 2019.

[17] Frank K. D. A., *Diffusion and Heat Transfer in chemical kinetics*. Plenum Press, New York, 1969.

[18] Makinde O. D., "Hermite-Padé approximation approach to thermal criticality for a reactive third-grade liquid in a channel with isothermal walls", *International Communications in Heat and Mass Transfer,* 34(7), 870–877, 2007.

[19] Guttamann A. J., *Asymptotic analysis of power –series expansions, Phase Transitions and Critical Phenomena*, C. Domb and J. K. Lebowitz, eds. Academic Press, New York, pp. 1—234, 1989.

[20] Hunter D. L. and Baker G. A., "Methods of series analysis III: Integral approximant methods", *Physical Review B*, vol. 19, pp. 3808—3821, 1979.